Journal of Materials Chemistry A

Accepted Manuscript

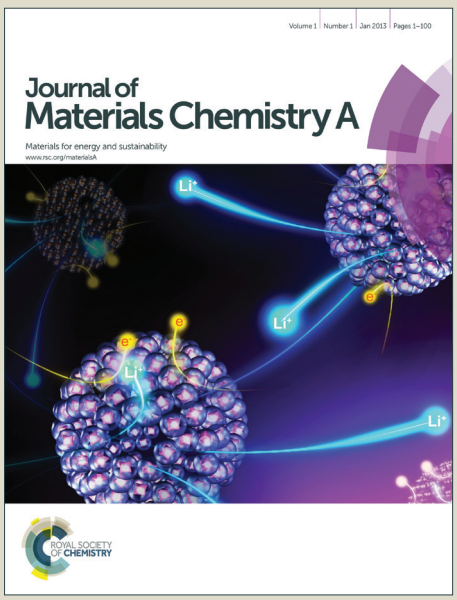

ROYAL SOCIETY OF CHEMISTRY

www.rsc.org/materialsA

Journal Name

RSCPublishing

ARTICLE

Development of Solvent-Free Hydrogen Storage and Release System based on Semi-Solid-State Ammonia Borane (AB) Fuel: High Gravimetric Capacity and Feasibility for Practical Application

Cite this: DOI: 10.1039/x0xx00000x

Sung-Kwan Kim,[a] Sung-Ahn Hong,[a] Ho-Jin Son,[a,*] Won-Sik Han,[c] Chang Won Yoon,[b] Suk Woo Nam,[b] and Sang Ook Kang[a,*]

Received ooth January 2012,
Accepted ooth January 2012

DOI: 10.1039/x0xx00000x

www.rsc.org/

Ammonia borane (AB), with high hydrogen contents and favorable dehydrogenation properties, is receiving intensive attention for its potential as the hydrogen storage materials. In this study, we demonstrates a new type of solvent-free AB fuel system to obtain a high hydrogen systemic gravimetric capacity needed for practical fuel cell application. The new storage material constitutes AB soaked in tetraethylene glycol dimethyl ether (TEGDE) with catalytic amount of palladium nanoparticles. Notably, TEGDE is very essential for the successful preparation of semi-solid state AB fuel system. The use of a minimum amount of TEGDE in this system allows the hybrid AB catalytic system to be fabricated as an efficient solvent and catalytic reaction medium, enabling a high gravimetric and volumetric capacity. For a real application, AB pellets with spherical shapes are manufactured by the co-precipitation of AB/TEGDE/PdNPs, followed by the compression of semi-solid AB fuel mixture for fuel transfer from fuel tank to the hydrogen generator. Consequently, this hybrid semi-solid state catalytic system exhibits a high gravimetric capacity of hydrogen [10.01 material weight%]. With a high hydrogen capacity, a high performance dehydrogenation is obtained as a result of synergistic effects facilitated by highly active PdNPs well-dispersed in the TEGDE medium.

Introduction

An on-board hydrogen storage system with a 5.5 total system weight (wt)%, enabling a 300 mile driving range, will be a milestone for the hydrogen economy.[1] Various hydrogen storage materials have been proposed and developed to meet the corresponding material-based gravimetric target of 9 mat. wt%.[2] Among other potential storage materials, aqueous $NaBH_4$ (H_2 source) with pressurized air as an oxidant has been used as the fuel for the proton-exchange membrane fuel cells (PEMFCs).[3] However, the practical limitation of $NaBH_4$-based system is the low system wt%[4]: the optimal concentration of $NaBH_4$ for maximum hydrogen is limited to 20 wt% (<2 wt% based on the system), because of the viscosity and low conversion efficiency at high concentration (>30 wt%). As shown in Equation 1, the consumption of water solvent by the produced $NaBO_2$ increases the solution viscosity. It, in turn, leads to a diffusion limitation in the contact between $NaBH_4$ and catalyst with a significant decrease of the hydrogen generation rate. For example, the high concentration (30 wt%) SBH (sodium borohydride) and conversion efficiency from $NaBH_4$ to H_2 (95%) are demanded for 4.5 system wt%. Therefore, new hydrogen storage materials for high gravimetric hydrogen storage capacity are necessary.

$$NaBH_4 + 2H_2O \rightarrow NaBO_2 \cdot xH_2O + 4H_2 + \text{heat } (x = 2 \text{ or } 4) \quad (1)$$

As an alternate material for hydrogen storage, ammonia borane (NH_3BH_3, AB) seems to be the most promising owing to its high gravimetric hydrogen storage capacity. AB possesses extremely high gravimetric and volumetric hydrogen density of 19.6 wt% and 0.145 kg H_2 L^{-1}, respectively, far exceeding the DOE 2015 target (9.0 wt% and 0.082 kg H_2 L^{-1}).[5]

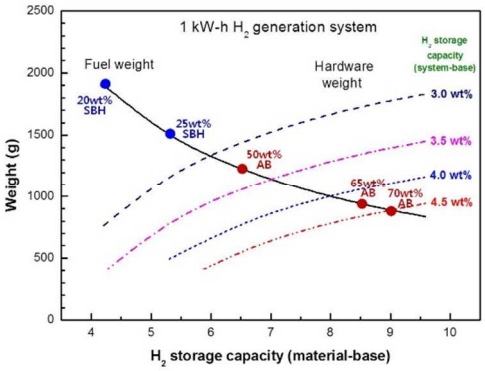

Fig. 1 A demand for AB or SBH ratio and H_2 storage capacity (material-base) for target of 4.5 system wt% target at 1 kW-h H_2 generation system.

With its high hydrogen density, AB is safe, nontoxic, chemically stable, easy to transport in its dry state, and highly soluble in water, enabling it to be used as a potential fuel for PEMFCs.[6] Homogeneous metal-catalyzed dehydrogenation is convenient and effective in harvesting hydrogen from AB. The drawback in this case

is the solvent contribution to the weight of the system, lowering overall hydrogen wt% of the system; 3.6 mat. wt% was estimated to be the maximum based on the best AB catalyst system developed to date.[7] To achieve the storage capacity over 9 mat. wt%, solid or semi-solid AB is suggested as the best option,[8] and the development of a heterogenous catalyst system is necessary.[9]

Neat AB can release H_2 in a stepwise thermolysis reaction. However, the practical application of AB is still inhibited by its slow thermal kinetics at <100 °C.[10] To lower the onset temperature, the use of nanoscaffolds,[11] ionic liquids,[12] and transition metals[13] was attempted. Autrey et al. reported the thermolysis of AB contained within mesoporous scaffolds. In his system, mesoporous silica decreased the thermolysis onset temperature by ~15 °C than that of neat AB.[14] Sneddon et al. reported the thermolysis of AB in minimal 1-butyl-3-methylimidazolium chloride which lowered the reaction onset temperature (versus solid AB) and increased dehydrogenation rate in the temperature range 85–95 °C.[15,16] Manners et al. also demonstrated that heterogeneous Rh(0) colloids (1.5 mol%) activated AB, releasing 2 equiv of H_2 to form borazine in tetraglyme at 45 °C in 72 h.[17]

In the course of developing an AB dehydrogenation catalyst, we recently reported that tetraethylene glycol (TG) derivative was not only a good solvent for AB dehydrogenation,[18a] but also an efficient growth source for the synthesis of metal nanoparticles (NPs). The TG-promoted route afforded size-controlled PdNPs, stabilizing against conglomeration without additional stabilizers. Consequently, the use of an atom-economical reagent, tetraethylene glycol dimethyl ether (TEGDE), enabled large-scale, one-pot production of PdNPs, which are very useful for practical fuel cell applications.

With such significance of PdNPs in hand, we focused on achieving the storage capacity target of 9 mat. wt% H_2 based on an AB semi-solid state system. To achieve the highest mat. wt% H_2 in the semi-solid state system featuring an AB/TEGDE/PdNP composite, minimal use of TEGDE is essential. The TEGDE-mediated PdNPs were applied for the generation of H_2 from AB/TEGDE semi-solid state system, resulting in a high capacity hydrogen storage system. For convenient fuel transfer from fuel tank to hydrogen generator and controllable H_2 release, the pellet type semi-solid material was manufactured by the developed "co-precipitation" method and subsequent compression of the AB/TEGDE/PdNPs mixtures. When the ratio of TEGDE/AB was adjusted to 35:65, the optimal performance of AB dehydrogenation with a high gravimetric capacity of H_2 (10.01 mat. wt%) was achieved. In this study, we describe a systematic investigation for the development of new type of hybrid hydrogen storage/release catalytic system based on AB material.

Experimental Section

Materials

All experiments were conducted under nitrogen atmosphere using Schlenk techniques or in an HE-493 dry box (Vacuum Atmosphere Co., Hawthorne, CA, USA). Ammonia borane was purchased from Aviabor (99%) and grounded to a free-flowing powder using a commercial coffee grinder. Tetraethylene glycol dimethyl ether (Tetraglyme, Alfa Aesar, 98+%), triethylene glycol and ethylene glycol dimethyl ether (Monoglyme, Sigma-Aldrich, 99%), triethylene glycol dimethyl ether (TGDE), diethylene glycol dimethyl ether (DGDE), ethylene glycol dimethyl ether (EGDE), tetraethylene glycol monomethyl ether (TEGME), tetraethylene glycol (TEG), and 3,6,9,12-tetraoxatridecanal (TEOTD) were purchased from Sigma-Aldrich and vacuum distilled over sodium under heating. Palladium acetate [$Pd_3(OAc)_6$] was purchased from Strem Chemicals Inc. The solvents tetraglyme and TEGDE were dried over Na, and methanol was distilled over CaH_2 under nitrogen.

Fabrication, Size Control, and Characterization of PdNPs

Large-scale one-pot surfactant-free synthesis of PdNPs was achieved by glycol ethers based on alkyl ethers of ethylene glycol: TEGDE, TGDE, DGDE, EGDE, TEGME, TEG, and TEOTD. The preparation of PdNPs from $Pd_3(OAc)_6$ in TEGDE **1**, TGDE **2**, DGDE **3**, EGDE **4**, TEGME **5**, TEG **6**, and TEOTD **7** solvents was performed at 140 °C. The PdNPs were synthesized by adding $Pd_3(OAc)_6$ (0.2 g, 0.3 mmol) to 20 mL of the solvent. These solutions were stirred at room temperature for 5 min under N_2 atmosphere for deoxygenation and further heated at 140 °C for 3 h. The color of the solution changed from orange to black, then the solution was cooled to room temperature. The product was separated by the centrifugation, and the solvent was removed by vacuum distillation. The resulting residues were washed with methanol (50 mL) twice, yielding black powders consisting of 3.6 (**1**), 4.7 (**2**), 6.1 (**3**), 5.9 (**4**), 50–100 (**5**), 10–15 (**6**), and 20–40 (**7**) nm particle size PdNPs.

Large-scale one-pot production of PdNPs

All reactions and handling were performed under a dry nitrogen atmosphere using standard Schlenk techniques including a vacuum system unless otherwise specified. For large-scale one-pot production of PdNPs, $Pd_3(OAc)_6$ (52.7 g, 234.9 mmol) was added to 800 mL of TG. The solutions were stirred for 5 min under N_2 atmosphere at room temperature, then heated at 140 °C for 3 h, followed by cooling them at room temperature. The color change from light brown to dark brown indicated the formation of palladium(0) nanoparticles. Black solutions containing Pd colloids were formed in this manner (see Fig. S3). The solvent was removed by vacuum distillation, and the resulting residue was washed twice with methanol (300 mL), yielding a black powder consisting of 4-nm PdNPs (20.5 g, 187.9 mmol) in 80% yield.

Kinetic profiles of Dehydrogenation of AB activated by Pd(0) nanoparticle catalysis

The concomitant dehydrogenation of AB was performed in a typical oil bath using a two-necked reaction flask connected to a water-filled cylinder glass tube. Hydrogen gas was released from semi-solid sate AB by the catalytic reaction, followed using a typical water-filled gas burette system, and the displaced volume of the water level in the gas burette was recorded every minute until no more hydrogen generation was observed. After complete hydrogen release, the reaction was stopped, and the reactor was seperated from the water-filled burette and disconnected from the water-filled tube with nitrogen purging, followed by releasing hydrogen pressure.

Preparation of AB/TEGDE/PdNPs pellet

All reactions were performed following standard Schlenk line techniques. AB (1.23 g, 40 mmol) was added to 30 mL monoglyme (ethylene glycol dimethyl ether) under a nitrogen

atmosphere. The resulting solution was stirred for at least 20 min. Then, for 30/70 TEGDE /AB pellet, TEGDE (0.66 g, density: 1.009 g mL^{-1}) was added to the AB solution; for 30/70 PdNPs + TEGDE/AB pellet, TEGDE (0.61 g) and PdNPs (0.05 g, 1.17 mol%) were added to the AB solution. The solution was stirred for at least 3 h at room temperature under nitrogen atmosphere. Then, the solvent was removed by vacuum distillation for 12 h, and the residual solvent was further removed by high vacuum (10^{-6} torr) for 3 h. AB/TEGDE and AB/TEGDE + PdNPs pellets were formed by the compression molding method. The AB/TEGDE/PdNPs powder (88 mg) was located in the mold cavity. Pressure was applied to force the material into contact with all mold areas, whereas the pressure was maintained until the molding material was cured. The pellets with spherical shape were removed from the mold cavity after AB dehydrogenation.

Analytical Methods

The PdNP samples were analyzed using field-emission transmission electron microscopy (TEM, FEI Tecnai F20). A very dilute solution of palladium(0) nanoparticle was redispersed in ethanol or hexane, and a drop of this solution was placed on the carbon curved copper grid for electron diffraction (ED) and energy-dispersive X-ray fluorescence spectroscopy (EDX). Powder XRD data were collected using a Rigaku D/MAX-2500 (18 kW) diffractometer. For the XRD measurements, the PdNP sample was dried, mixed with 325-mesh Si powder, and placed on a Si wafer sample holder. TGA study was performed using a TGA/DSC 1 (Mettler-Toledo Inc.) thermogravimetric analyzer. For TGA study, sample mass was limited to <2–3 mg, because AB/TEGDE/PdNPs, AB/TEGDE, and AB have a tendency to significantly expand in the volume during the pyrolysis, which may cause an obstacle on the TGA profile or a contact with the internal wall of the TGA furnace. Therefore, TGA was conducted, and the data were confirmed several times. The sample was loaded into a weight tared alumina pan, and heated at a rate of 5 °C min^{-1} from 25 to 180 °C under flowing nitrogen (50 mL min^{-1}). DSC experiments were performed using a DSC 1 system (Mettler-Toledo incorporated). AB/TEGDE/PdNPs, AB/TEGDE, and AB were weighed in an aluminum pan, which was then crimped. A pinhole allowed the escape of the evolved gases. The samples were heated at a heating rate of 5 °C min^{-1} from 25 °C to 180 °C under N_2 purging (50 mL min^{-1}), after an initial 30 min isothermal period at 40 °C for removing atmospheric gases and adsorbed moisture. Both instruments were calibrated in the studied temperature 25–180 °C min^{-1}. Solution NMR spectra were recorded at room temperature using a Mercury-300BB spectrometer (Varian Inc., Palo Alto, CA, USA), unless otherwise stated. The spectral frequency was 96.3 MHz for ^{11}B, and NMR shifts in ppm are reported with reference to external standards of $BF_3{\cdot}Et_2O$ for the ^{11}B nucleus.

Results and discussion

TG derivatives as an essential additive for high performance PdNPs catalyst preparation: the structural optimization of TG derivatives by varying alkyl chain length and type of terminal group

Previously, we reported TG derivative as an efficient growth source for producing PdNPs.[18b] The large-scale one-pot TG-mediated PdNPs preparation is an efficient and convenient method in the absence of surfactant. Approximately 20 g of PdNPs was synthesized in a single reaction; however, in most other known NP syntheses, only subgram quantities have been produced. Further investigation on the effect of TG moiety was investigated by systematic structural and alkyl chain length control for the optimization of the PdNPs synthesis. For this study, the PdNPs were freshly prepared from a series of ethylene glycol derivatives with different alkyl chain length [n = 4, TEGDE; n = 3, triethylene glycol dimethyl ether (TGDE); n = 2, diethylene glycol dimethyl ether (DGDE); and n = 1, ethylene glycol dimethyl ether (EGDE)]. The TEM images and particles size distributions of the glymes are shown in Fig. 2. The particles size decreases with increasing glymes chain length, indicating that particle size depends on chain length (–$(OCH_2CH_2)_n$–). EGDE, DGDE, TGDE, and TEGDE additives formed 5.9, 6.1, 4.7, and 3.6 nm size PdNPs, respectively, with narrow particle size distributions.

(a)

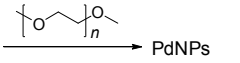

EGDE = Ethylene glycol dimethylether
DGDE = Diehtylene glycol dimethyl ether
TGDE = Triethylene glycol dimethyl ether
TEGDE = Tetraethylene glycol dimethyl ether

(b)

n	NP size (nm)	Viscosity (mm^2/s)
1 (EGDE)	5.9	0.5
2 (DGDE)	6.1	1.2
3 (TGDE)	4.7	2.5
4 (TEGDE)	3.6	4.1

Chart 1 a) Synthesis of PdNPs from $Pd(OAc)_2$ precursor in different glymes. b) Viscosities of glymes and sizes of PdNPs prepared from different glymes.

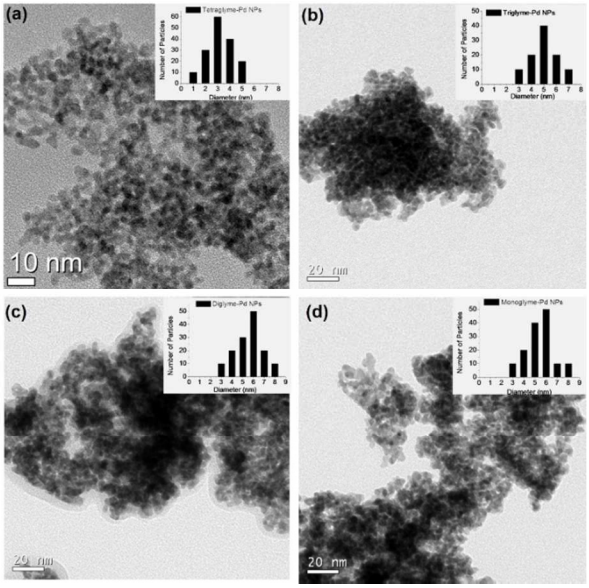

Fig. 2 TEM images and particles size histograms of PdNPs from a) TEGDE, b) TGDE, c) DGDE, and d) EGDE.

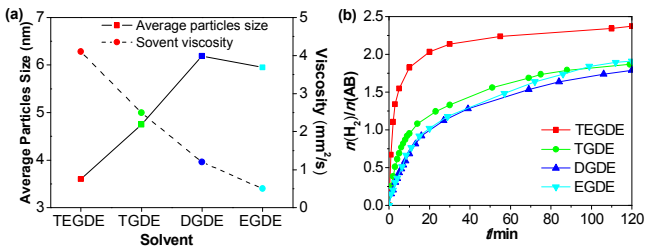

Fig. 3 a) The effects of glymes chain length and solvent viscosity on PdNPs size. b) The effect of PdNPs size on catalytic activity for AB dehydrogenation.

Such trend can be interpreted as a result of different mass transfer rate of both the reducing agent and Pd^{2+}, affecting the

formation and growth rate of PdNPs. Naturally, the extent of mass transfer is closely related to the degree of solvent viscosity. Indeed, the solvent viscosity increases with glymes chain length (4.1 (TEGDE) > 2.5 (TGDE) > 1.2 (DGDE) > 0.5 (EGDE) mm^2/s at 20 °C).[19] The variation in the viscosity as a function of type of glymes is plotted with the change of the particle size as shown in Fig. 3a. The correlation showed a good agreement with the previous report,[20] demonstrating that the viscosity of the medium is a crucial factor affecting the aggregation of nanoparticles. TG group only controls the particle size in these systems (any other reagent except tetraethylene glymes (TG) group is not used); therefore, the solvent viscosity is indicated to be a key parameter that affects the aggregation of nanoparticles. A theoretical analysis also explains that the solvent viscosity is a key parameter affecting the particle size, thus determining the morphology of particles during the nanoparticle synthesis in the solution.[21] The catalytic activities of the controlled-size PdNPs prepared in TEGDE, TGDE, DGDE, and EGDE were tested and compared. PdNPs (**1**, TEGDE) with particle size of 3.6 nm showed the best catalytic performance than PdNPs (**2**, TGDE), PdNPs (**3**, DEGE), and PdNPs (**4**, EDGE) with 4.8, 6.2, and 5.9 nm particle sizes, respectively, (Fig. 3b) and released 1.5 equiv of H_2 in 5 min and 2 equiv of H_2 in 20 min at 80 °C for the first and second equivalents of hydrogen released, respectively.

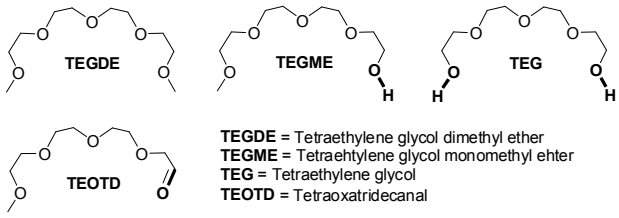

Chart 2 Molecular structures of TEGDE and its substituents.

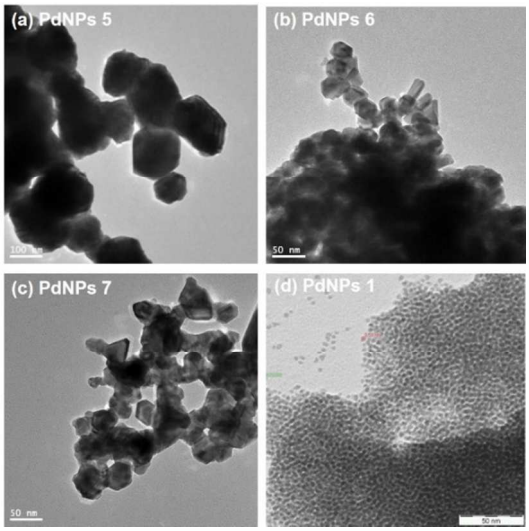

Fig. 4 TEM images of PdNPs (**5**–**7** and **1**) prepared in TEGME **5**, TEG **6**, TEOTD **7** and TEGDE **1** [Scale bar: 100 nm for a); 50 nm for b), c), and d)].

For further study on the substituent effect, three different functional moieties viz., carboxylic acids, aldehydes, and hydroxyl functional groups, which are generally used as a common additive in nanocrystal syntheses for improving the reproducibility of growth rates and size control,[22] were investigated as the terminal group of the TG derivatives. A series of tetraethylene glycol ether substituents having different terminal functional groups such as tetraethylene glycol monomethyl ether (TEGME), tetraethylene glycol (TEG), and 3,6,9,12-tetraoxatridecanal (TEOTD) were prepared as shown in Chart 2.

Each PdNPs was synthesized from the prepared TEGME, TEG, TEOTD, and TEOTDA additives to check the functional group effect on the AB dehydrogenation kinetics. Fig. 4 shows the TEM images of the prepared PdNPs. The PdNPs **5**–**7** prepared from TEGME, TEG, and TEOTD, respectively, revealed much bigger particle size in the range 50–100 nm with more structural pattern than ~4 nm particle size of PdNPs **1** synthesized from TEGDE, indicating that all the functionalized TG moieties other than TEGDE does not efficiently prevent the aggregation of the PdNPs (Fig. 4). Their catalytic activities were also tested and compared to the parent PdNPs **1**. The relatively poor catalytic activities of the PdNPs **5**–**7** than that of **1** were consistent with their similar dehydrogenation performances (see Fig. S1 in Supporting Information). A poor catalytic behavior can be simply explained in terms of the general size-dependence of transition metal catalysts (activity–particle size relationship), indicating that the rate of catalytic reaction increases with decreasing particle size.[23] This comparison clearly indicates that the small particle size of the PdNPs effectively accelerate the dehydrogenation efficiency. Consequently, among various PdNPs **1**–**7** prepared from different oligoethylene glycol ethers, 4 nm particle size of PdNPs **1** was selected and used for the fabrication and optimization of semi-solid system.

Optimization of AB:TEGDE ratio for improvement of gravimetric density (material weight percent, mat. wt%)

With highly active 4 nm PdNPs **1** synthesized in TEGDE, we focused on achieving the storage capacity target of 9 mat. wt% H_2 based on an AB semi-solid state system. To obtain a high mat. wt% H_2 in the semi-solid state system, a minimum amount of TEGDE was used as a solvent and catalytic reaction medium. The effect of TG weight on mat. wt% H_2 and PdNPs kinetics with the AB is listed in Table 1.

Table 1 Effect of TEGDE weight percentage on mat. wt% and PdNPs kinetics with AB[a)]

Entry	TEGDE wt%	AB wt%	Equiv of H_2	Time (min)	Mat. wt%[b)]
1	25	75	1.59	120	7.75
2	30	70	1.81	120	8.26
3	35	65	2.37	120	10.01
4	40	60	1.99	120	7.78
5	50	50	1.18	120	3.82

[a)]General conditions: 0.123 g AB, 80 °C, PdNPs **1** (0.005 g, 1.17 mol%); [b)]Mat. wt% = released H_2-wt./(AB+TEGDE+PdNPs-wts.).

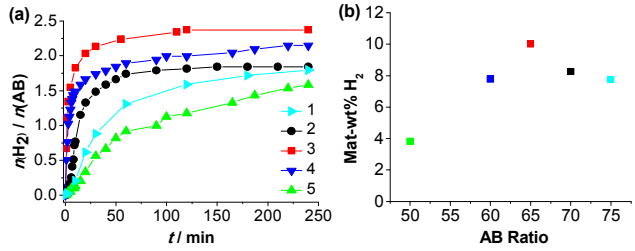

Fig. 5 a) AB dehydrogenation kinetic profiles by PdNPs in TEGDE. AB:TEGDE ratio [**1** (75:25), **2** (70:30), **3** (65:35), **4** (60:40), and **5** (50:50)] at 80 °C. b) Mat. wt% measurements of the reaction with different AB:TEGDE ratio at 80 °C.

AB (1.23 g) was used to optimize the TG amounts. The optimal amount of TG was 0.3 g (25:75 TG/AB mixture, 10.7 mat. wt% H_2), and it significantly enhanced mat. wt% H_2 and H_2 release rates when compared to 0.15 g (12:88 TG/AB, 7.2 mat. wt% H_2), 0.5 g (40:60 TG/AB, 6.1 mat. wt% H_2), and 1.0 g (80:20 TG/AB, 1.1 mat. wt% H_2) TG systems (Fig. 3a). Pseudo first-order rate constants of 0.4×10^{-3} s^{-1} (0.15 g), 6.7×10^{-3} s^{-1} (0.3 g TG), 1.7×10^{-3} s^{-1} (0.5 g TG), and 0.5×10^{-3} s^{-1} (1.0 g TG) were obtained from logarithmic plots (Fig. 8b).[24] When these conditions were applied to the generation of H_2 from AB, the highest capacity H_2 storage system of 10.7 mat. wt% H_2 was achieved (Entry 2 in Table 1). Fig. 5b shows that the dehydrogenation reaction of AB/TEGDE with PdNPs reveals unexpected results, but a favorable concentration dependence. A decrease in mat. wt% in 40:60 and 50:50 TEGDE/AB ratios results from lower diammonate of diborane $[BH_2(NH_3)_2]^+[BH_4]^-$ (DADB) concentration than that of 35:65 ratio. The relative amounts of both DADB and *B*-(cyclodiborazanyl)aminoborohydride (*cyc*$[NH_2BH_2NH_2BH]$-NH_2BH_3, BCDB) as AB dehydrogenation intermediates formed during the thermal decomposition increased in highly concentrated solutions.[25] A decreases in mat. wt% in 25:75 and 30:70 TEGDE/AB ratios is attributed to the solid-state case of the AB and a mixing problem of AB with TEGDE.

The manufacture of semi-solid state pellets composed of AB, TEGDE, and PdNPs mixture for fuel cell application

Materials applicable for chemical hydrogen storage are available in a variety of forms including pure-component liquids (cyclohexane,[1a] decaline,[26] and *n*-ethylcarbazole[27]), solutions (low concentration aqueous sodium borohydride[4] and AB in diglyme[9f] or THF[6b]), slurries (high concentration aqueous sodium borohydride[4] and magnesium or lithium hydride in oil[28]), and solids (AB).[29] These different classes of materials have been processed in diverse ways. Most liquid systems involve the use of a catalytic reactor for hydrogen release, and moving the fuel within the system is achieved using pumps similar to those used in gasoline-powered vehicles. The most significant difference from the traditional fueling systems is in the case of processing solids or slurries. Slurries can be difficult because the formulation is not optimized to keep particle suspended in the flow and can damage the catalyst and clog the system. For solid chemical storage materials, the use of catalysts for hydrogen release is mostly prohibitive, because the catalyst would have to be incorporated into the fuel formulation, enhancing the reaction rates at lower temperature and greater fuel instability in the storage tank. It is more likely that hydrogen would be released thermally from solid chemical hydrogen storage systems or a second reagent is blended with the fuel to enable release of hydrogen as needed.

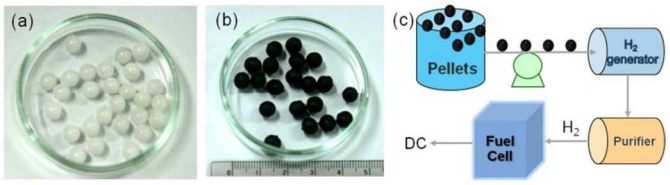

Fig. 6 Photo image of a) AB pellet and b) AB/TEGDE/PdNPs pellet (AB:TEGDE ratio= 70:30, 1.17 mol% PdNPs), and c) schematics of configurations with transfer of pellets.

In this study, we combined solid and liquid systems for their synergistic effect on semi-solid state system. A solid AB is blended with a small amount of TEGDE and highly active Pd nanocatalysts. The appeal of a system operating in this manner is the pelletizing of materials (molding AB/TEGDE/PdNPs to a shape of pellet). For these semi-solids, less gravimetric penalty exists, but void volume in the pellet bed represents a significant volumetric penalty. To overcome this problem and reduce void volume, the packing in close-packed spheres was used as shown in Fig. 6.[30]
The co-precipitation method by introducing 1.17 mol% PdNPs based on the catalyst to AB with a small amount of TEGDE in the semi-solid was investigated. AB (60 mg, 1.95 mmol) was added to TEGDE (monoglyme), and after dissolving AB, the pellets composed of AB:TEGDE with 65:35 ratio, TEGDE (30 mg), and PdNPs (2 mg, 1.17 mol%) were added to the AB solution. After mixing and drying of TEGDE-soaked AB/PdNPs, AB/TEGDE/PdNPs pellets were formed by the compression molding. A small pellet (92 mg) was capable of storing relatively large quantities of hydrogen (0.1 L) in a very small volume mixture. Fig. 6c shows the schematics of the configurations with transfer of pellet in fuel tank from pellet tank to H_2 generator.[30]

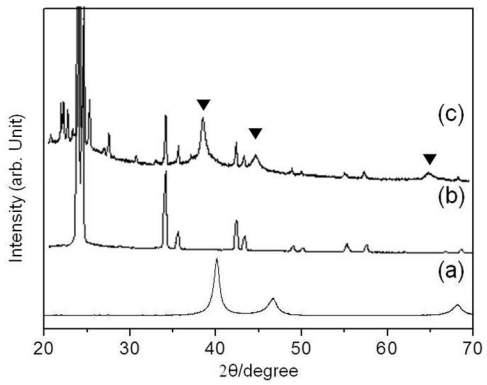

Fig. 7 XRD patterns of a) PdNPs, b) AB, and c) AB/TEGDE/PdNPs pellet. ▼ Diffraction peaks of palladium hydride (Pd–H).

The X-ray diffraction (XRD) patterns of AB/TEGDE/PdNPs pellet, PdNPs, and commercial AB are shown in Fig. 7. The typical diffraction peaks of AB are also observed in AB/TEGDE/PdNPs (curve C), revealing that AB (JCPDS No. 74-0894) exists as the crystalline phase in the mixed sample. The newly generated peaks in the range ~20–30° can be explained as a result of interaction between TEGDE and PdNPs. Interestingly, when AB is mixed with TEGDE, the typical diffraction patterns of PdNPs at 40, 46, and 68° (JCPDS No. 87-0637) disappeared, whereas three distinct peaks defining as Pd–H species appeared at 38, 45, and 65° (JCPDS No. 65-0057). These observations is in well agreement with that the dehydrogenation from AB is proceeded by the abstraction of H atoms from AB by PdNPs at low temperature, indicating that the Pd–H species play an important role in destabilizing AB.

Table 2 TGA results of AB/TEGDE/PdNPs, AB/TEGDE, and AB/PdNPs.

Entry	Total weight loss per unit weight of sample (wt%)	Total weight loss per unit weight of AB (wt%)[a)]
A	35.4	50.6
B	36.2	55.7
C	11.6	12.0
D	35.2	50.3
E	35.9	55.2
F	36	36

[a)]The weight loss per unit weight of AB is calculated according to the following equation: total weight loss per unit weight of AB = [(total wt. loss of AB/TEGDE or AB/TEGDE/Pd or AB/Pd) / (AB ratio 70 or 65%).

The thermal properties of the AB/TEGDE/PdNPs pellets were tested and compared by thermogravimetric analysis (TGA). The following samples were examined: AB/TEGDE/PdNPs (65:35),

AB/TEGDE/PdNPs (70:30), AB/TEGDE (65:35), AB/TEGDE (70:30), AB/PdNPs, and neat AB. The total weight losses of these sample when heating from room temperature to 180 °C are listed in Table 2. To check the effect of PdNPs on AB dehydrogenation, TGA was performed for AB/PdNPs samples. The TGA curve of AB/PdNPs (curve C in Fig. 8a) shows three temperature regimes as follows: 3.0%, 5.0%, 3.6% weight losses in the ranges ~50–100 °C (regime 1); 100–120 °C (regime 2); and ~120–180 °C (regime 3), respectively. The total weight loss of sample C is ~11.6 %. The TGA of AB in the presence of TEGDE was also measured to investigate the role of TEGDE on AB dehydrogenation. The TGA data of AB/TEGDE and sample E (AB:TEGDE, 65:35) show two temperature regimes as follows: 1.4% and 34.5% weight losses in the ranges ~30–100 °C (regime 1) and ~100–180 °C (regime 2), revealing a total weight loss of ~35.9% for neat AB. Meanwhile, for the TGA curve of neat AB (curve F in Fig. 8a), the significant weight loss started at relatively higher temperatures (>100 °C): 14.9%, 1.1%, and 20% weight losses in the ranges ~100–122 °C (regime 1), ~122–136 °C (regime 2), and ~136–180 °C (regime 3), indicating that both the PdNPs and TEGDE promotes AB decomposition. Interestingly, when AB was mixed with TEGDE and PdNPs, the decomposition of AB was accelerated. As shown in Fig. 8a, these AB/TEGDE/PdNPs samples (samples A and B) showed high reaction rates at lower temperature (even at below 50 °C): sample B (AB:TEGDE, 65:35) with PdNPs revealed 9.0% weight loss in the range ~30–100 °C (regime 1), besides 19.2% and 8.0% weight losses in the ranges ~100–140 °C (regime 2) and ~140–180 °C (regime 3), respectively. Sample A (AB:TEGDE, 70:30) with PdNPs also showed the similar feature to sample B; however, a slightly larger AB content in the sample A decreased loss of total mass than that of sample B.

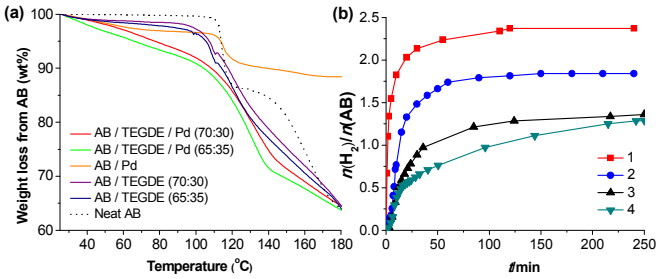

Fig. 8 a) TGA results of AB/TEGDE/PdNPs, AB/TEGDE, and AB/PdNPs. The heating rate is 5 °C min^{-1}. b) AB dehydrogenation kinetic profiles based on the TGA data [**1** AB/TEGDE/PdNPs, 65:35; **2** AB/TEGDE/PdNPs, 70:30; **3** AB/TEGDE, 65:35; **4** AB/TEGDE 70:30] at 80 °C.

To elaborate TGA results and evaluate the amount of PdNPs taken part in the activation of AB dehydrogenation, as shown in Fig. 8b, the dehydrogenation of AB semi-solid fuels in different ratio was performed to compare the kinetic profiles of AB/TEGDE fuels with or without PdNPs. A 20 min measurement time maximized the difference among the fuel ratios with or without PdNPs. Without PdNPs, AB/TEGDE dehydrogenations was sluggish even at 80 °C, only giving off 0.28 and 0.53 equiv H_2 in 20 min in 70:30 and 65:35 AB/TEGDE ratios, respectively, and proceeded to the completion with a total H_2 amounts of 1.17 equiv in 120 min. However, the PdNPs participation was noticeable in the dehydrogenation kinetics for 70:30 fuel ratio of AB/TEGDE: during initial 20 min time span, 1.3 equiv H_2 was released, 1.7 equiv H_2 in 60 min, and finally subsided with 1.8 equiv H_2 in 250 min. The optimal H_2 liberation was accomplished at a fuel ratio of 65:35 for AB/TEGDE with PdNPs by releasing 2.0 and 2.3 equiv of H_2 in 20 and 60 min time intervals, respectively, and finally subsided with 2.4 equiv H_2 in 250 min. From these experiments, the mixing of both PdNPs and TEGDE in the hybrid AB system significantly increased AB dehydrogenation kinetics for AB/TEGDE semi-solid fuels, regardless of the fuel ratios at temperatures <100 °C.

A noticeable difference derived from the synergetic effect is also observed by differential scanning calorimetry (DSC). Fig. 9 shows the DSC curves of AB/TEGDE/PdNPs: (A) AB/TEGDE/PdNPs (65:35), (B) AB/TEGDE/PdNPs (70:30), (C) AB/Pd, (D) AB/TEGDE (70:30), (E) AB/TEGDE (65:35), and (F) neat AB. The DSC exothermal onset temperatures (T_{on}), peak temperatures (T_p), and exothermic enthalpies (ΔH) of these three samples are listed in Table 3.

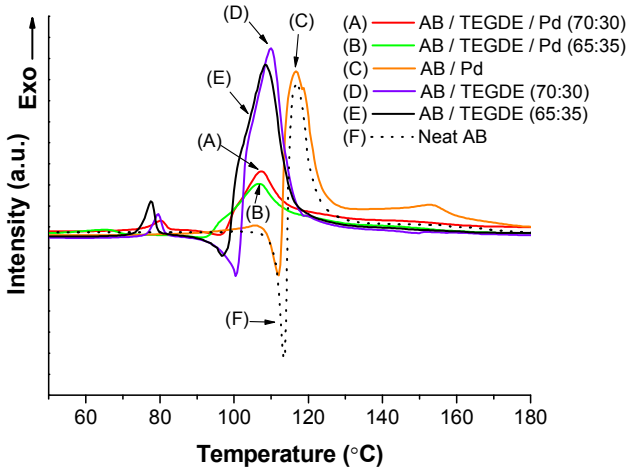

Fig. 9 DSC results of AB/TEGDE/PdNPs, AB/TEGDE, and AB/PdNPs. The heating rate is 5 °C min^{-1}.

Table 3 DSC T_{on}, T_p, and exothermic ΔH data of AB/TEGDE/PdNPs, AB/TEGDE, and AB/PdNPs.

Entry	T_{on1} (°C)	T_{p1} (°C)	ΔH_1 (J(g-AB)$^{-1}$)	T_{on2} (°C)	T_{p2} (°C)	ΔH_2 (J(g-AB)$^{-1}$)	ΔH_{total} (J(g-AB)$^{-1}$)
A	75	80	52.27	98	107	878.27	930.54
B	50	65	49.37	93	107	942.75	992.12
C	98	105	25.55	113	118	856.69	882.24
D	76	79	36.43	101	111	776.16	812.59
E	74	77	56.85	98	109	899.52	956.37
F	-	-	-	111	118	1309.64	1309.64

First, neat AB (curve F) revealed the relatively big endothermic and exothermic peaks over the temperature ranges 110–115 and 120–160 °C, respectively. A significant change in ΔH and high T_{on} can be interpreted as a result of a compromise between the endothermic process required to break hydrogen bonds between AB molecules/to melt the neat AB solid and the exothermic reaction derived from AB decomposition. However, such big peaks and high T_{on} were decreased significantly and lowered by adding PdNPs or TEGDE. As shown in Fig. 9, the endothermic peaks C, D, E, and F have much smaller peak size and lower temperature than neat AB (F), indicating the weakened hydrogen bonding interaction between AB molecules. Notably, the decreasing and lowering trends were maximized when AB was mixed with TEGDE and PdNPs. Curves A and B show significantly smaller value of the second exothermic peak than others (neat AB, only Pd mixture, and only TEGDE mixture), and their thermal decomposition (hydrogen releasing) temperature decreased <100 °C. The relieved enthalpy change also shows a relationship with the gentle (gradual) downhill of the TGA curves for AB/TEGDE/PdNPs samples over broad temperature range (30–180 °C). For convenience, the changes in the enthalpy per

unit weight of AB (i.e., ΔH_{total}/g-AB) are included in Table 3 with DSC data. In turn, such gentle change in enthalpy as a function of temperature can be a significant advantage in real fuel cell application, which is necessary for the controllable hydrogen releasing system and stability of the AB fuel that would be improved under the mild condition.

Conclusion

In summary, we demonstrated that the use of TEGDE for the development of the AB dehydrogenation catalytic system is an effective pathway to obtain high gravimetric capacity and enhance the dehydrogenation kinetics. TEGDE plays not only as the most suitable element for PdNPs preparation, but also as an effective medium for good miscibility in heterogeneous multi-components (AB, TEGDE, and PdNPs), significantly improving the dehydrogenation kinetics. When TEGDE-mediated PdNPs was applied for the generation of H_2 from AB/TEGDE semi-solid state system with 35:65 ratio of TEGDE/AB, the high hydrogen storage system {10.01 mat. wt% [mat. wt% = H_2-wt./(AB+ TG + PdNPs-wts.)]} was achieved with the optimal performance of AB dehydrogenation completing hydrogen release in 20 min at 80 °C. For building a convenient fuel transfer and controllable H_2 release for the practical application such as potential long-endurance and long-range fuel cell unmanned aerial vehicle, we manufactured a small size of pellet material (AB/TEGDE/PdNPs), confirming that this hybrid system provides various advantages for improvement in the gravimetric and volumetric capacity of hydrogen storage materials with the synergistic effect obtained in the disparate combination of AB, highly active PdNPs, and TEGDE. Efforts toward mechanistic investigation and performance optimization of the AB catalytic system utilizing different types of transition metal NPs are currently underway.

Acknowledgements

This work was supported by the New & Renewable Energy Core Technology Program of the Korea Institute of Energy Technology Evaluation and Planning(KETEP) granted financial resource from the Ministry of Trade, Industry & Energy, Republic of Korea (No. 20113030040020).

Notes and references

[a] Department of Advanced Materials Chemistry, Korea University, Sejong 339-700, Korea.
[b] Fuel Cell Center, Korea Institute of Science and Technology, Hawolgok-dong 39-1, Seongbuk-gu, Seoul 136-791, Korea.
[c] Department of Chemistry, Seoul Women's University, Hwarang-ro 621, Seoul, Korea.

† Electronic Supplementary Information (ESI) available: AB dehydrogenation kinetics by PdNPs prepared in **1**, **5**, **6**, **7**, TEM images of PdNPs, and photoimage showing large-scale one-pot production of PdNPs. See DOI: 10.1039/b000000x/

1 (*a*) L. Schlapbach and A. Züttel, *Nature* 2001, **414**, 353; (*b*) T. Q. Hua, R. K. Ahluwalia and J.-K. Peng, Technical assessment of compressed hydrogen storage tank systems for automotive applications (DOE has recently lowered the 2015 gravimetric total system target to only 5.5 total system wt%), http://www1.eere.energy.gov/hydrogenandfuelcells/pdfs/compressedtank_storage.pdf, accessed: September, 2014.

2 (*a*) S. Satyapal, J. Petrovic, C. Read, G. Thomas and G. Ordaz, *Catal. Today* 2007, **120**, 246; (*b*) K. C. Ott, 2009 Overview – DOE Chemical Hydrogen Storage Center of Excellence (CHSCoE), http://www.hydrogen.energy.gov/pdfs/progress09/iv_b_1a_ott.pdf, accessed: September, 2014.

3 (*a*) H. I. Schlesinger, H. C. Brown, A. E. Finholt, J. R. Gilbreath, H. R. Hockstra and E. K. Hyde, *J. Am. Chem. Soc.* 1953, **75**, 215; (*b*) B. Sen and C. M. Kaufman, *J. Chem. Soc. Dalton Trans.* 1985, **64**, 307.

4 S. J. Kim, J. Lee, K. Y. Kong, C. R. Jung, I.-G. Min, S.-Y. Lee, H.-J. Kim, S. W. Nam and T.-H. Lim, *J. Power Sources* 2007, **170**, 412.

5 S. Satyapal, J. Petrovic, C. Read, G. Thomas and G. Ordaz, *Catal. Today* 2007, **120**, 246.

6 (*a*) Y. S. Chen, J. L. Fulton, J. C. Linehan and T. Autrey, *J. Am. Chem. Soc.* 2005, **127**, 3254; (*b*) M. C. Denney, V. Pons, T. J. Hebden, D. M. Heinekey and K. I. Goldberg, *J. Am. Chem. Soc.* 2006, **128**, 12048; (*c*) Q. Xu and M. Chandra, *J. Power Sources* 2006, **163**, 364; (*d*) C. W. Yoon and L. G. Sneddon, *J. Am. Chem. Soc.* 2006, **128**, 13992; (*e*) T. J. Clark, G. R. Whittell and I. Manners, *Inorg. Chem.* 2007, **46**, 7522; (*f*) F. H. Stephens, V. Pons and R. T. Baker, *Dalton Trans.* 2007, 2613.

7 N. Blaquiere, S. Diallo-Garcia, S. I. Gorelsky, D. A. Black and K. Fagnou, *J. Am. Chem. Soc.* 2008, **130**, 14034.

8 (*a*) D. J. Heldebrant, A. Karkamkar, N. J. Hess, M. Bowden, S. Rassat, F, Zheng, K. Rappe and T. Autrey, *Chem. Mater.* 2008, **20**, 5332; (*b*) M. E. Bluhm, M. G. Bradley, R. Butterick III, U. Kusari and L. G. Sneddon, *J. Am. Chem. Soc.* 2006, **128**, 7748.

9 (*a*) W. R. H. Wright, E. R. Berkeley, L. R. Alden, R. T. Baker and L. G. Sneddon, *Chem. Commun.* 2011, **47**, 3177; (*b*) S. S. Mal, F. H. Stephens and R. T. Baker, *Chem. Commun.* 2011, **47**, 2922; (*c*) F. Cheng, H. Ma, Y. Li and J. Chen, *Inorg. Chem.* 2007, **46**, 788; (*d*) S. D. Benedetto, M. Carewska, C. Cento, P. Gislon, M. Pasquali, S. Scaccia and P. P. Prosini, *Thermochimica Acta,* 2006, **441**, 184; (*e*) S. B. Kalidindi, J. Joseph and B. R. Jagirdar, *Energy Environ. Sci.* 2009, **2**, 1274; (*f*) R. P. Shrestha, H. V. K. Diyabalanage, T. A. Semelsberger, K. C. Ott and A. K. Burrell, *Int. J. Hydrogen Energy* 2009, **34**, 2616; (*g*) Ö. Metin, S. Duman, M. Dinç and S. Özkar, *J. Phys. Chem. C* 2011, **115**, 10736.

10 (*a*) V. Sit, R. A. Geanangel and W. W. Wendlandt, *Thermochim. Acta* 1987, **113**, 379; (*b*) G. Wolf, J. Baumanna, F. Baitalowa and F. P. Hoffmann, *Thermochim. Acta* 2000, **343**, 19.

11 (*a*) H. Kim, A. Karkamkar, T. Autrey, P. Chupas and T. Proffen, *J. Am. Chem. Soc.* 2009, **131**, 13749; (*b*) A. Paolone, O. Palumbo, P. Rispoli, R. Cantelli, T. Autrey and A. Karkamkar, *J. Phys. Chem. C* 2009, **113**, 10319; (*c*) S. Sepehri, A. Feaver, W. J. Shaw, C. J. Howard, Q. Zhang, T. Autrey and G. Cao, *J. Phys. Chem. B* 2007, **111**, 7469.

12 D. W. Himmelberger, L. R. Alden, M. E. Bluhm and L. G. Sneddon, *Inorg. Chem.* 2009, **48**, 9883.

13 (*a*) I. G. Green, K. M. Johnson and B. P. Roberts, *J. Chem. Soc., Perkin Trans. 2* 1989, 1963; (*b*) C. A. Jaska, K. Temple, A. J. Lough and I. Manners, *J. Am. Chem. Soc.* 2003, **125**, 9424; (*c*) T. He, Z. Xiong, G. Wu, H. Chu, C. Wu, T. Zhang and P. Chen, *Chem. Mater.* 2009, **21**, 2315.

14 A. Gutowska, L. Li, Y. Shin, C. M. Wang, X. S. Li, J. C. Linehan, R. S. Smith, B. D. Kay, B. Schmid, W. J. Shaw, M. Gutowski and T. Autrey, *Angew. Chem. Int. Ed.* 2005, **44**, 3578.

15 (*a*) D. W. Himmelberger, C. W. Yoon, M. E. Bluhm, P. J. Carroll and L. G. Sneddon, *J. Am. Chem. Soc.* 2009, **131**, 14101; (*b*) P. J. Fazen, E. E. Remsen, J. S. Beck, P. J. Carroll, A. R. McGhie and L. G. Sneddon, *Chem. Mater.* 1995, **7**, 1942; (*c*) P. J. Fazen, J. S. Beck, A. T. Lynch, E. E. Remsen and L. G. Sneddon, *Chem. Mater.* 1990, **2**, 96.

16 L. G. Sneddon, Ammoniaborane Hydrogen Storage – New Methods for Promoting Amineborane Dehydrogenation/Regeneration Reactions, http://www.hydrogen.energy.gov/pdfs/progress07/iv_b_5e_sneddon.pdf, accessed: September, 2014.

17 (*a*) C. A. Jaska, K. Temple, A. J. Lough and I. Manners, *Chem. Commun.* 2001, 962; (*b*) C. A. Jaska and I. Manners, *J. Am. Chem. Soc.* 2004, **126**, 9776; (*c*) C. A. Jaska, T. J. Clark, S. B. Clendenning, D. Grozea, A. Turak, Z.-H. Lu and I. Manners, *J. Am. Chem. Soc.* 2005, **127**, 5116.

18 (*a*) S.-K. Kim, W.-S. Han, T.-J. Kim, T.-Y. Kim, S. W. Nam, M. Mitoraj, Ł. Piękoś, A. Michalak, S. J. Hwang and S. O. Kang, *J. Am. Chem. Soc.* 2010, **132**, 9954; (*b*) S.-K. Kim, T.-J. Kim, T.-Y. Kim, G. Lee, J. T. Park, S. W. Nam and S. O. Kang, *Chem. Commun.* 2012, **48**, 2021.

19 CLARIANT.com, http://www.glymes.clariant.com/bu/ics/internet.nsf/vwWebPagesByID/0D177AE294830930C1257ABE003E778D?OpenDocument, accessed: September, 2014.

20 (*a*) S. Matsuo and T. Makita, *Int. J. Thermophys.* 1989, **10**, 833; (*b*) M. J. Assael and S. K. Polimatidou, *Int. J. Thermophys.* 1994, **15**, 95; (*c*) J. A. Jacob, S. Kapoor, N. Biswas and T. Mukerjee, *Colloids and Surfaces A: Physicochem. Eng. Aspects* 2007, **301**, 329; (*d*) Y. Huang, J. Liao, C. Liu, T. Lu and W. Xing, *Nanotechnology* 2009, **20**, 105604.

21 G. Oskam, *J. Sol–Gel Sci. Techn.* 2006, **37**, 161.

22 F. Wang, R. Tang and W. E. Buhro, *Nano Lett.* 2008, **8**, 3521.

23 R. A. Van Santen, *Acc. Chem. Res.* 2009, **42**, 57.

24 M. Käß, A. Friedrich, M. Drees and S. Schneider, *Angew. Chem. Int. Ed.* 2009, **48**, 905.

25 J. F. Kostka, R. Schellenberg, F. Baitalow, T. Smolinka and F. Mertens, *Eur. J. Inorg. Chem.* 2012, 49.

26 S. Hodoshima, H. Arai, S. Takaiwa and Y. Saito, *Int. J. Hydrogen Energy* 2003, **28**, 1255.

27 G. P. Pez, A. R. Scott, A. C. Cooper, H. Cheng, F. C. Wilhelm and A. H. Abdourazak, US 7351395, 2008.

28 (*a*) P. M. Irving, W. L. Allen and T. Healey, presented at 2000 Hydrogen Program Annual Review Meeting, Novel Catalytic Reforming Using Microtechnology with Advanced Separation Technology, San Ramon (California, USA), May 9-11, 2000; (*b*) D. Mori and K. Hirose, *Int. J. Hydrogen Energy* 2009, **34**, 4569.

29 C. L. Aardahl and S. D. Rassat, *Int. J. Hydrogen Energy* 2009, **34**, 6676.

30 Y. Kim, Y. Kim, S. Yeo, K. Kim, K. J.-E. Koh, J.-E. Seo, S. J. Shin, D.-K. Choi, C. W. Yoon and S. W. Nam, *J. Power Sources* 2013, **229**, 170.

New hydrogen storage material (pellet type semi-solid) shows the high-performance dehydrogenation with its high gravimetric capacity (10.01 mat. wt%).